JOURNAL OF AGRICULTURAL AND FOOD CHEMISTRY

Article

pubs.acs.org/JAFC

More on the Losses of Dissolved CO_2 during Champagne Serving: Toward a Multiparameter Modeling

Gérard Liger-Belair,*[,†,‡] Maryline Parmentier,[‡] and Clara Cilindre[†,‡]

[†]Equipe Effervescence, Groupe de Spectrométrie Moléculaire et Atmosphérique, UMR CNRS 7331, UFR Sciences Exactes et Naturelles, Université de Reims Champagne-Ardenne, BP 1039, 51687 Reims Cedex 2, France

[‡]Laboratoire d'Œnologie et Chimie Appliquée, URVVC UPRES EA 4707, UFR Sciences Exactes et Naturelles, Université de Reims Champagne-Ardenne, BP 1039, 51687 Reims Cedex 2, France

ABSTRACT: Pouring champagne into a glass is far from being inconsequential with regard to the dissolved CO_2 concentration found in champagne. Three distinct bottle types, namely, a magnum bottle, a standard bottle, and a half bottle, were examined with regard to their loss of dissolved CO_2 during the service of successively poured flutes. Whatever the bottle size, a decreasing trend is clearly observed with regard to the concentration of dissolved CO_2 found within a flute (from the first to the last one of a whole service). Moreover, when it comes to champagne serving, the bottle size definitely does matter. The higher the bottle volume, the better its buffering capacity with regard to dissolved CO_2 found within champagne during the pouring process. Actually, for a given flute number in a pouring data series, the concentration of dissolved CO_2 found within the flute was found to decrease as the bottle size decreases. The impact of champagne temperature (at 4, 12, and 20 °C) on the losses of dissolved CO_2 found in successively poured flutes for a given standard 75 cL bottle was also examined. Cold temperatures were found to limit the decreasing trend of dissolved CO_2 found within the successively poured flutes (from the first to the last one of a whole service). Our experimental results were discussed on the basis of a multiparameter model that accounts for the major physical parameters that influence the loss of dissolved CO_2 during the service of a whole bottle type.

KEYWORDS: *champagne, sparkling wines, carbonated beverages, carbonation, dissolved CO_2, champagne service, diffusion*

INTRODUCTION

From a strictly chemical point of view, Champagne wines are multicomponent hydroalcoholic systems, with a density close to unity, a surface tension $\gamma \approx 50$ mN m^{-1} (indeed highly ethanol dependent), and a viscosity about 50% larger than that of pure water (also mainly due to the presence of 12.5% v/v ethanol).[1] Champagne and sparkling wines elaborated through the *méthode traditionnelle* also hold dissolved carbon dioxide (CO_2) gas molecules, formed together with ethanol during a second fermentation process (called prise de mousse and promoted by adding yeasts and sugar inside bottles filled with a base wine and sealed with a cap). Actually, because bottles are sealed, CO_2 molecules produced by yeasts cannot escape and progressively dissolve into the wine. This is an application of Henry's law which states that the concentration of a dissolved gas is proportional to its partial pressure in the vapor phase.[1−3] Champagne therefore holds a concentration of dissolved CO_2 proportional to the level of sugar added in the base wine to promote this second fermentation. Traditionally, 24 g of sugar per liter (g L^{-1}) is added in the base wine to promote the prise de mousse, and a standard Champagne wine holds close to 12 g L^{-1} of dissolved CO_2, which corresponds to a volume close to 5 L of gaseous CO_2 per each standard 75 cL bottle (under standard conditions for temperature and pressure). No wonder champagne tasting mainly differs from still wine tasting due to this amount of dissolved CO_2.

Carbonation or the perception of dissolved CO_2 involves a truly very complex multimodal stimulus. During champagne tasting, dissolved CO_2 acts on both trigeminal receptors[4−8] and gustatory receptors[9,10] in addition to the tactile stimulation of mechanoreceptors in the oral cavity (through bursting bubbles). For recent and global overviews of how dissolved CO_2 may promote chemically induced sensations in the oral and nasal cavities, see the review by Brand[11] and the most recent edition of the book by Lawless and Heymann.[12] Moreover, a link has been recently evidenced between carbonation and the release of some aroma compounds in carbonated waters.[13,14] Sensory results revealed that the presence of CO_2 increased aroma perception in mint-flavored carbonated beverages.[14] Dissolved CO_2 therefore leads to modifications of the neuro-physicochemical mechanisms responsible for aroma release and flavor perception in carbonated beverages. Following these recent highlights, it seems therefore pertinent to keep the dissolved CO_2 molecules as long as possible inside the liquid phase during champagne tasting. Champagne wine elaborators, as well as sommeliers, progressively become aware of trying to propose to clients and consumers an ideal way of keeping and serving champagne.

After uncorking a bottle of champagne, dissolved CO_2 can escape from the liquid phase into the form of bubbles, provided that immersed particles or defects of the glass wall are able to entrap tiny air pockets (larger than a critical size) which may therefore act as bubble nucleation sites.[15,16] It is the so-called effervescence process. Nevertheless, it is worth noting that inside the bottle most of the immersed particles (including, for

Received: May 18, 2012
Revised: October 8, 2012
Accepted: October 30, 2012
Published: October 30, 2012

example, yeast cells and tartaric acid crystals) are rendered harmless as a result of soaking during aging in the closed bottle. Moreover, CO_2 molecules also inevitably escape by "invisible" diffusion through the free air/champagne interface.[1−3] In a standard flute poured with champagne, it was found that for every one CO_2 molecule which escapes from champagne into the form of bubbles approximately four others directly escape by invisible diffusion through the free air/champagne interface.[17] Invisible diffusion is therefore undoubtedly the main pathway as concerns the loss of dissolved CO_2 during champagne and sparkling wine tasting. During the past decade, a large body of research has been devoted to bubble nucleation, bubble rise, and bubble collapse, under standard champagne tasting conditions.[18] Nevertheless, and to the best of our knowledge, the pouring step has been very poorly investigated. Actually, during the service of champagne, the bottle progressively inclines from a vertical to a roughly horizontal position. The free air/champagne interface offered to invisible losses of dissolved CO_2 from champagne therefore considerably increases. Moreover, this almost horizontal position, characteristic from champagne serving, and which provides the largest possible air/champagne area within the bottle (with regard to the champagne volume), is kept until the last flute has been filled (see Figure 1). Continuous and invisible losses of dissolved CO_2 are therefore strongly suspected during the service of a whole bottle (from the first flute to the last one).

Figure 1. During champagne serving, the bottle is kept almost horizontal, which provides the largest possible air/champagne area offered to invisible losses of dissolved CO_2 from the champagne bulk within the bottle. (Photograph by Jean-Marie Lecomte/collection CIVC.)

In this article, concentrations of dissolved CO_2 found in successively poured flutes were reported during the service of a given whole champagne bottle type (from the first to the last flute). Three distinct bottle types, namely, a magnum bottle, a standard bottle, and a half bottle, were examined with regard to their respective loss of dissolved CO_2 during the service of successively poured flutes. The impact of champagne temperature on the losses of dissolved CO_2 found in successively poured flutes was also examined. Moreover, a multiparameter model was built, which provides the progressive decline of dissolved CO_2 found in successively poured flutes, during the service of a whole bottle type.

MATERIALS AND METHODS

Temperature Dependence of Champagne Viscosity. A standard commercial Champagne wine, recently elaborated with a blend of 100% chardonnay base wines (vintage 2009; Cooperative Nogent l'Abbesse, Marne, France), was used for this set of experiments. Since their elaboration, bottles were stored in a cool cellar, at 12 °C. Under standard temperature conditions for champagne tasting (usually from 5 to 15 °C), the viscosity of champagne is known to be strongly temperature dependent. The temperature dependence of champagne viscosity, as measured with a thermostatted Ubelhode capillary viscosimeter (with a sample of champagne first degassed), was found to classically obey the following Arrhenius like eq 1

$$\eta(T) \approx 1.08 \times 10^{-7} \exp\left(\frac{2.81 \times 10^3}{T}\right) \quad (1)$$

where the dynamic viscosity η is expressed in kg m^{-1} s^{-1} (i.e., in Pa s) and the temperature T is expressed in K.

Three Various Bottle Types. The standard commercial Champagne wine used for this set of experiments was elaborated and corked in bottles of various shape and volume content. The three most commonly used bottle types were investigated with regard to their respective loss of dissolved CO_2 during the service of successively poured flutes: namely, the standard bottle (with a champagne volume of 75 cL), the magnum bottle (with a champagne volume of 150 cL), and the half bottle (with a champagne volume of 37.5 cL). It is worth noting that these three various bottles present indeed different volume content but the same headspace volume (denoted v_{HS}) of 25 mL as well as similar cork stoppers (in terms of length and cross section). It is also worth noting that champagne was elaborated with 24 g/L of sugar added in the base wine to promote the prise de mousse, whatever the bottle type, so that the same amount of about 12 g/L of CO_2 was initially produced into each bottle type. This was definitely a crucial condition in order to correctly compare the three various bottle types against each other with regard to their respective loss of dissolved CO_2 during the service of successively poured flutes.

Initial Concentration of Dissolved CO_2 in Each Bottle Type. Generally speaking, the solubility of a given gas into a solution is strongly temperature dependent (the lower the temperature of the solution, the higher the gas solubility). Agabaliantz thoroughly examined the solubility of dissolved CO_2 (i.e., its Henry's law constant) as a function of both temperature and wine parameters.[19] Thermodynamically speaking, the behavior of the Henry's law constant as a function of temperature can be conveniently expressed with a Van't Hoff like equation as follows[2]

$$k_H(T) = k_{298K} \exp\left[-\frac{\Delta H_{diss}}{R}\left(\frac{1}{T} - \frac{1}{298}\right)\right] \quad (2)$$

where k_{298K} is the Henry's law constant of dissolved CO_2 at 298 K (~1.21 g L^{-1} bar^{-1}), ΔH_{diss} is the dissolution enthalpy of CO_2 molecules in the liquid medium (in J mol^{-1}), R is the ideal gas constant (8.31 J K^{-1} mol^{-1}), and T is the absolute temperature (in K). By fitting Agabaliantz data with the latter equation, the dissolution enthalpy of CO_2 molecules in champagne was evaluated (see Figure 2).[2] The best fit to Agabaliantz data was found with $\Delta H_{diss} \approx 24\,800$ J mol^{-1}.

Because the solubility of CO_2 strongly depends on the champagne temperature, as shown in Figure 2, the partial pressure of gaseous CO_2 under the cork also strongly depends, in turn, on the champagne temperature. The physicochemical equilibrium of CO_2 molecules within a champagne bottle is ruled by both Henry's law and the ideal gas law (for the gaseous CO_2 trapped in the headspace under the cork). Moreover, because bottles are hermetically closed, conservation of the total mass of CO_2 within the bottle (dissolved into the wine and in the vapor phase) applies. Therefore, by combining Henry's law and the ideal gas law with mass conservation, the following relationship was derived, which links the partial pressure P of gaseous CO_2 under the cork (in bars) with both temperature and the bottle's parameters[3]

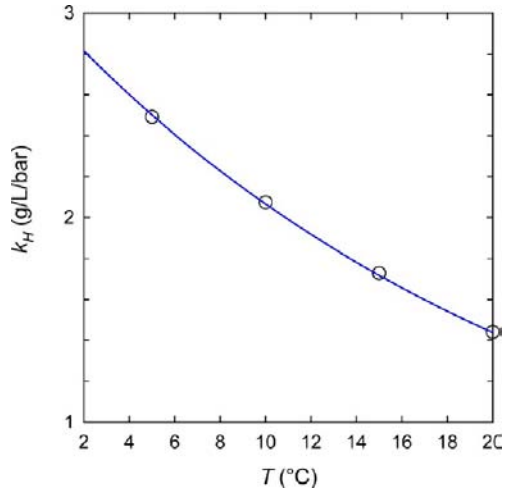

Figure 2. Henry's law constant as a function of temperature (○); redrawn from Agabaliantz data;[19] dashed line is the best fit to Agabaliantz data, drawn with the Van't Hoff like eq 2 and with $\Delta H_{diss} \approx 24\,800$ J mol^{-1}.[2]

$$P \approx \frac{mRT}{4.4 \times 10^3 v_{HS} + k_H RTV} \quad (3)$$

It is worth noting that eq 3 was specifically engineered in order to use the given parameters in the standard unities usually used in enology. m is the total mass of CO_2 within the bottle (in g), T is the champagne temperature (in K), k_H is the (temperature-dependent) solubility of CO_2 given in eq 2 (in g L^{-1} bar^{-1}), V is the volume of champagne within the bottle (in L), and v_{HS} is the volume of the gaseous headspace under the cork (in L). The prefactor 4400 in the denominator originates from the conversion factor and from the molar mass of CO_2 (i.e., 44 g mol^{-1}). Moreover, since dissolved and gaseous CO_2 experience equilibrium through Henry's law, the concentration of dissolved CO_2 found within the closed bottle (in g L^{-1}) expresses as follows[3]

$$c_0 = k_H P \approx \frac{k_H mRT}{4.4 \times 10^3 v_{HS} + k_H RTV} \quad (4)$$

The temperature dependence of the initial dissolved CO_2 concentration found within champagne, for the three aforementioned bottle types, is displayed in Figure 3. It can be seen from Figure 3 that the smaller the bottle volume, the lower the initial concentration of dissolved CO_2 (despite the same sugar level of 24 g L^{-1} added in the base wine to promote the prise de mousse). It is also worth noting that the concentration of dissolved CO_2 is rather slightly temperature dependent, despite a pressure within the bottle which is highly temperature dependent in this range of temperatures.[3]

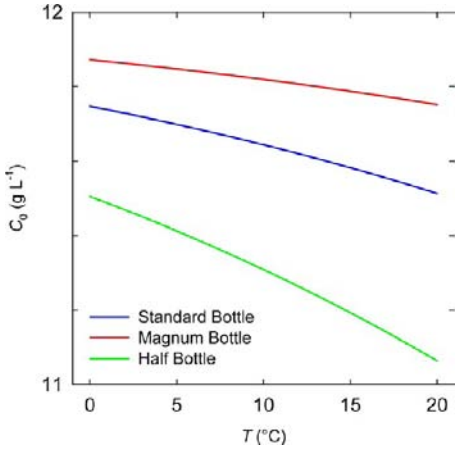

Figure 3. Temperature dependence of the initial dissolved CO_2 concentration found within champagne (elaborated within the three corked bottle types).

Batch of Flutes and Their Washing Protocol. Series of identical flutes (namely, long-stemmed glasses with a deep tapered bowl and a narrow aperture) were used for this set of experiments. In order to avoid the randomly located "bubbling environment" inevitably provided in glasses showing natural effervescence, we decided to serve champagne in flutes etched on their bottom, such as those used in recent papers.[20−22] Between the successive pourings and data recordings, flutes were thoroughly washed in a dilute aqueous formic acid solution, rinsed using distilled water, and then compressed air dried. This drastic treatment forbids formation of calcium carbonate crystals on the flute wall as well as adsorption of any dust particle acting as "natural" bubble nucleation sites, so that bubble nucleation is strictly restricted to ring-shaped etching, thus providing a standardized effervescence. By pouring champagne into such glasses (standardized with regard to their bubbling behavior), differences in concentrations of dissolved CO_2 between successively poured flutes during the serving of a whole bottle (from the first to the last flute) are therefore attributed only to losses of dissolved CO_2 experienced from the champagne "reservoir" found inside the bottle. Flutes were stored at room temperature (∼20 ± 1 °C).

Service Protocol. After uncorking a given bottle type, a volume of 100 ± 4 mL of champagne was successively served into a number of flutes depending on each bottle type. Fourteen flutes were successively served with a magnum bottle, whereas seven flutes and only three flutes were successively served for the standard and half bottle type, respectively. During the service of a whole given bottle type, the successively poured flutes were horizontally aligned, close to each others on a table, so that champagne vertically falls and hits the bottom of each flute (thus providing a thick head of foam, which quickly vertically extends, and then progressively collapses, as illustrated in Figure 4). Once a flute was filled with champagne, another flute was immediately served, and so on, until the last flute was filled. Approximately 10 s was needed to fill a flute. Between the services of successive flutes, the bottle was kept as horizontal as possible in order to avoid turbulences of the champagne interface. This way is the traditional way of serving champagne and sparkling wines in bars, clubs, and restaurants.

Impacts on the losses of dissolved CO_2 between the successively poured flutes from a standard 75 cL bottle were investigated for three sets of champagne temperatures, namely, 4, 12, and 20 °C. It is worth noting that as the heat capacity of the glass (∼0.8 kJ kg^{-1} K^{-1}) is much lower than that of champagne (∼4.2 kJ kg^{-1} K^{-1}), the temperature of champagne remains almost constant during the few seconds of the pouring process.[23]

Measuring Concentrations of Dissolved CO_2 in the Successively Poured Flutes. Concentrations of dissolved CO_2 found in the successively poured flutes were determined using carbonic anhydrase (labeled C2522 Carbonic Anhydrase Isozyme II from bovine erythrocytes and provided from Sigma-Aldrich). This is the official method recommended by the OIV (namely, the International Office of Vine and Wine) for measuring the dissolved CO_2 concentration in Champagne and sparkling wines.[24] This method is thoroughly detailed in a paper by Liger-Belair et al.[25] Measurements of dissolved CO_2 concentrations in each flute were carried out immediately after having poured champagne in the flute (to prevent a loss of dissolved CO_2 due to the progressive and ineluctable diffusion of gaseous CO_2 into the form of bubbles and from the air/champagne interface). To enable a statistical treatment, five successive pourings and dissolved CO_2 measurements were done for each bottle type at 12 °C and four successive pourings at 4 and 20 °C. An arithmetic average of the data provided by the successive pourings was taken to finally produce one single "average" dissolved CO_2 concentration corresponding to a given flute number, served from a given bottle type, at a given temperature.

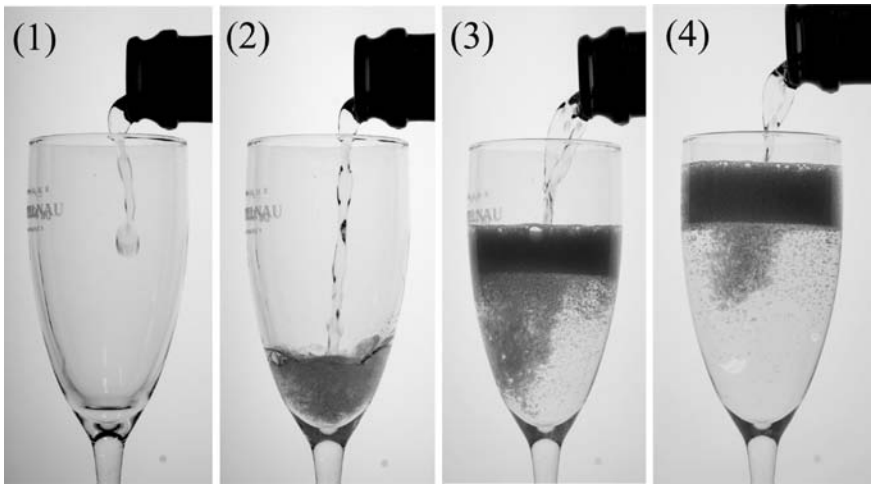

Figure 4. Time sequence illustrating the pouring process; this way of pouring champagne is the traditional way of serving champagne and sparkling wines in bars, clubs, and restaurants. (Photographs by Gérard Liger-Belair.)

Statistical Analysis. Statistical analysis was done by Student's *t* test (two-tailed, two-sample unequal variance) to determine whether average concentrations of dissolved CO_2 were considered as statistically different from one pouring condition to another.

Modeling the Desorption of Dissolved CO_2. Molecular diffusion is actually the mechanism behind the progressive desorption of dissolved gas species from the free surface area of a supersaturated liquid medium (as dissolved CO_2 molecules continuously do from the free air/champagne interface, once the bottle is uncorked). The number of CO_2 moles that cross the air/champagne interface per unit of time (by molecular diffusion) is ruled by

$$\left(\frac{dn}{dt}\right)_D = \iint_{\substack{\text{air/champagne}\\ \text{interface}}} \vec{J} \times d\vec{S} \tag{5}$$

where $\vec{J}$ is the flux of CO_2 moles defined by the first Fick's law, $\vec{J} = -D\vec{\nabla}c$. In the latter equation, D is the diffusion coefficient of CO_2 molecules in the liquid phase and $\vec{\nabla}c$ is the gradient of CO_2 dissolved moles between the champagne bulk and the air/champagne interface in equilibrium with the gaseous CO_2 in the vapor phase outside the liquid phase.

By assuming a linear gradient of dissolved CO_2 between the champagne bulk and the air/champagne interface, $\vec{\nabla}c$ may be rewritten as $-\Delta c/\delta$, with δ being the thickness of the boundary layer where a gradient of dissolved CO_2 exists, and $\Delta c = c_L - c_i$ is the difference in dissolved CO_2 concentrations between the liquid bulk (denoted c_L) and the air/champagne interface (denoted c_i) in equilibrium with the gaseous CO_2 in the vapor phase. After uncorking the bottle and during the pouring process, ambient air progressively invades the bottle to replace the liquid which escapes through the bottleneck (see Figure 5). The partial pressure of gaseous CO_2 in ambient air being on the order of only 0.0004 bar (since the natural abundance of CO_2 in the ambient air is close to 400 ppm) and the solubility of CO_2 in champagne being on order of 1.5 g L^{-1} bar^{-1} at 20 °C, the equilibrium CO_2 concentration expresses as $c_i = k_H P_{CO_2} = 1.5 \times 4 \times 10^{-4} \approx 0.6$ mg $L^{-1} \ll c_L$. Therefore, $\Delta c = c_L - c_i \approx c_L$.

Generally speaking, desorption of dissolved gas species is ruled by pure diffusion or diffusion–convection whether the supersaturated liquid medium is perfectly stagnant or in motion.[26] In the case of a liquid medium agitated with flow patterns, convection forbids the growing of the diffusion boundary layer by supplying the liquid near the free surface with dissolved gas molecules freshly renewed from the liquid bulk.[26] Pouring champagne into a flute is a turbulent process, which induces formation of various eddies and convection currents through the liquid phase. Therefore, loss of dissolved CO_2 from champagne during the pouring step is undoubtedly ruled by diffusion–convection, and the boundary layer where a gradient of dissolved CO_2 exists is considered as being constant. Finally, by developing, eq 5 can be rewritten as follows

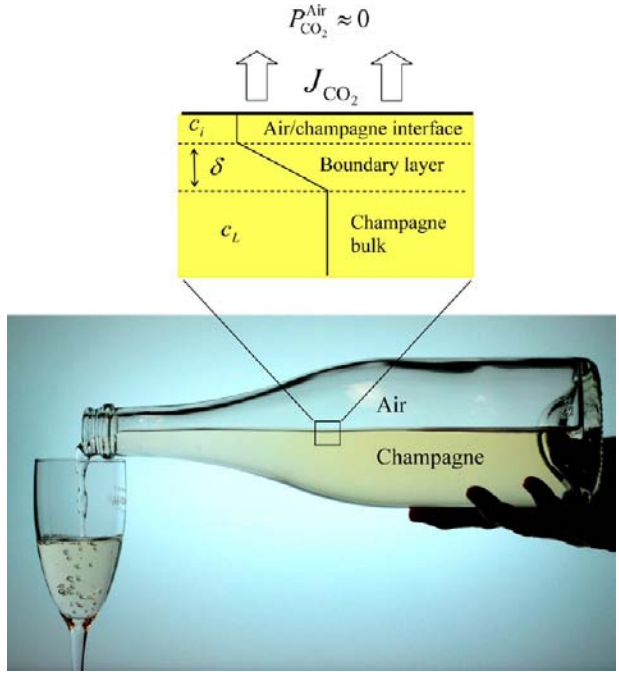

Figure 5. Photograph showing the flat air/champagne interface during the pouring step, and scheme of the surface boundary layer where a gradient of dissolved CO_2 exists. (Photograph by Gérard Liger-Belair.)

$$\left(\frac{dn}{dt}\right)_D \approx -DS\frac{c_L}{\delta} \tag{6}$$

with S being the area of the air/champagne interface offered to molecular diffusion.

The total number of dissolved CO_2 moles within the champagne bulk found inside the bottle being expressed as $n = c_L V$ (with V being the champagne bulk volume), eq 6 therefore transforms as

$$\left(\frac{dn}{dt}\right)_D = V\left(\frac{dc_L}{dt}\right) \approx -DS\frac{c_L}{\delta} \tag{7}$$

Actually, during the pouring process, the volume V of champagne inside the bottle evolves. It obviously constantly decreases as time proceeds since champagne escapes from the bottleneck to

progressively invade the flute. As the velocity at which champagne is poured into a flute being considered is constant during the pouring process (the time needed to progressively pour 100 mL of champagne into a flute is of order of 10 s), the volume of champagne remaining in the bottle is expressed as

$$V(t) \approx V_0 - kt \tag{8}$$

with V_0 being the initial volume of champagne within the bottle, before pouring (in cm^3), k being the rate at which champagne escapes from the bottleneck during the pouring process (i.e., $k = -dV/dt$, in cm^3 s^{-1}), and t being the time (in s).

The total number of dissolved CO_2 moles within the champagne bulk found in the bottle can therefore be accessed through the following equation

$$\left(\frac{dn}{dt}\right)_T = \frac{d}{dt}(c_L V) = c_L\frac{dV}{dt} + V\frac{dc_L}{dt} \tag{9}$$

Combining the latter equation with eqs 7 and 8 leads to the following relationship

$$\left(\frac{dn}{dt}\right)_T = -c_L k - Vk\frac{dc_L}{dV} \approx -c_L k - DS\frac{c_L}{\delta} \tag{10}$$

By simplifying, the latter equation transforms as

$$\frac{dc_L}{c_L} \approx \frac{dV}{V}\left(\frac{DS}{k\delta}\right) \tag{11}$$

The scheme displayed in Figure 6 compiles the pertinent geometrical parameters of the model. For modeling purposes, the surface S of the

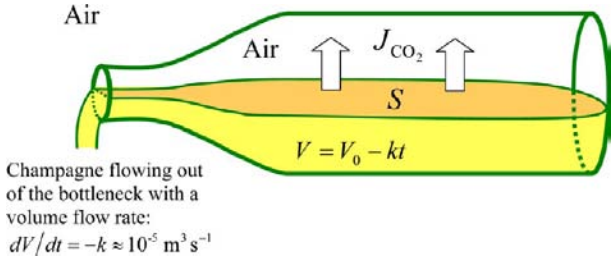

Figure 6. Scheme which compiles the various geometrical pertinent parameters used in our model; S is the air/champagne interface offered to invisible dissolved CO_2 diffusion from the champagne bulk within the bottle, whereas V is the time-dependent volume of champagne remaining within the bottle during the pouring process.

air/champagne interface offered to gaseous CO_2 diffusion during the pouring process is considered as constant in the following and equates the largest possible air/champagne area when the bottle is half full. By integrating eq 11 and by considering (for modeling purposes) S, k, and δ as being roughly constant during the pouring process, the following relationship is deduced

$$\frac{c_L}{c_0} \approx \left(\frac{V}{V_0}\right)^{(DS/k\delta)} \tag{12}$$

with c_0 and V_0 being the initial concentration of dissolved CO_2 found within the champagne bulk (before pouring) and the initial volume of champagne within the bottle, respectively, and V being the volume of champagne remaining within the bottle.

RESULTS AND DISCUSSION

Concentrations of Dissolved CO_2 Found within the Successively Poured Flutes Depending on the Bottle Type. Concentrations of dissolved CO_2 data, as chemically measured immediately after having successively poured champagne into each flute (from the first to the last flute), are displayed in Figure 7 for each bottle type served at 12 °C. Each flute is labeled by a number n corresponding to its place in

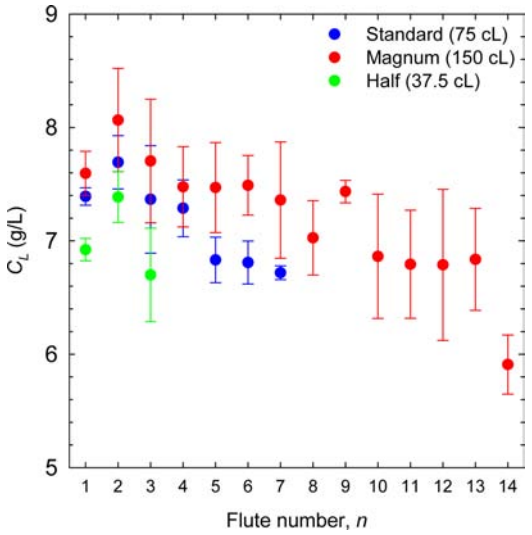

Figure 7. Concentrations of dissolved CO_2 data found within each flute number successively filled from a single bottle (from the first to the last flute) for each bottle type served at 12 °C; each data is the arithmetic average of the values provided from the successive data series; error bars represent the 95% confidence interval.

the series of successive pouring: namely, from 1 to 14 for the magnum bottle, from 1 to 7 for the standard bottle, and from 1 to 3 for the half bottle, respectively.

Generally speaking, concentrations of dissolved CO_2 found within the flutes are well below those found within the bottle (before pouring). This observation, consistent with a recent article, is the result of the loss of dissolved CO_2 happening during the pouring process (mainly due to turbulences and bubble entrapment when champagne invades the flute during the pouring process).[25] It was indeed observed that champagne loses between 3 and 4 g/L of dissolved CO_2 after having been poured in a flute standing vertically (depending on its temperature). Moreover, and despite significant error bars, a decreasing trend is clearly observed with regard to the concentration of dissolved CO_2 found within a flute (from the first to the last one of a whole service). Furthermore, it is also worth noting from Figure 7 that, for a given flute number in a data series, the concentration of dissolved CO_2 found within the flute decreases as the bottle volume decreases. For example, the third flute served from a given bottle type holds a concentration of dissolved CO_2 higher in the magnum (~7.7 g L^{-1}) than in the standard bottle (~7.4 g L^{-1}), which also holds a concentration of dissolved CO_2 higher than in the half bottle (~6.7 g L^{-1}). The trend becomes indeed statistically significant from the fifth flute between the magnum and the standard bottle. For the standard and half bottle, respectively, concentrations of dissolved CO_2 within the first and third flute were statistically different (with $P < 0.01$ and 0.1, respectively). Finally, the comparison between the magnum and the half bottle provides concentrations of dissolved CO_2 statistically different (with $P < 0.01$ for the first flute, and $P < 0.1$ for the second and third flute).

Concentrations of Dissolved CO_2 Found within the Successively Poured Flutes Depending on the Champagne Temperature. Concentrations of dissolved CO_2 data,

as chemically measured immediately after having successively poured champagne into each flute (from the first to the last flute), are displayed in Figure 8 for standard 75 cL bottles

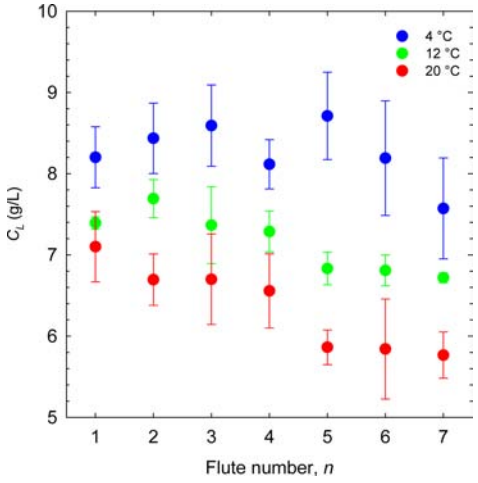

Figure 8. Concentrations of dissolved CO_2 data found within each flute number successively filled from a single bottle (from the first to the last flute), for standard 75 cL bottles, and for the three champagne temperatures (i.e., 4, 12, and 20 °C); each data is the arithmetic average of the successive values provided from the successive data series; error bars represent the 95% confidence interval.

served at three temperatures (i.e., 4, 12, and 20 °C). It is worth noting from Figure 8 that for a given flute number in a data series the concentration of dissolved CO_2 found within the flute decreases as the champagne temperature increases. Statistical analysis confirmed differences in the concentrations of dissolved CO_2, for a given flute number, between the champagne served at 20 and 4 °C (with $P < 0.01$) and between the champagne served at 12 and 4 °C (with $P < 0.05$ for the six firsts flutes, and $P < 0.1$ for the last one). Significant differences between 12 and 20 °C were observed for all flutes ($P < 0.05$), except for the first ($P > 0.1$) and third flute ($P \approx 0.1$). Moreover, the decreasing trend observed with regard to the concentration of dissolved CO_2 found within the successively poured flutes (from the first to the last one of a whole service) is all the more important as the champagne temperature increases. The differences in dissolved CO_2 concentrations between the first and the last flute served are ~0.6 g L^{-1} for a champagne served at 4 °C, ~0.7 g L^{-1} for a champagne served at 12 °C, and ~1.3 g L^{-1} for a champagne served at 20 °C.

Nevertheless, despite a general decreasing trend in dissolved CO_2 concentration from the first to the last flute served, we were surprised to notice in Figures 7 and 8 (at 4 and 12 °C) that c_L actually increases at first and does not follow the expected trend. We are aware that extreme data (outliers) may skew the average, but we nevertheless propose a tentative hypothesis based on the so-called onomatopoeic "glug−glug" effect.[27] Actually, the emptying of a horizontal bottle (initially full of liquid, surrounded by air, and submitted to the action of gravity) reveals that the liquid first flows rather chaotically out of the bottle, through a succession of jets of liquid and admissions of air bubbles. This effect is all the more important that the bottle is full of liquid. As soon as there is enough air into the bottle indeed, the liquid flows smoothly, without this very characteristic glug−glug effect. As concerns champagne serving, the glug−glug effect exists during the pouring of (i) the two first flutes for the standard bottle, (ii) the four first flutes for the magnum bottle, and (iii) only the first flute of the half-bottle. Whatever the bottle type, the first flute served is therefore always subjected to a more chaotic flow, which inexorably accelerates the loss of dissolved CO_2 concentration through turbulences and bubble entrapment. More experiments specifically dealing with the service of flutes experiencing the glug−glug effect are nevertheless required to conclude about the seemingly lower dissolved CO_2 concentrations found in the first served flutes, whatever the bottle type. Moreover, regarding the greater loss of dissolved CO_2 of the earlier flutes, it is not unusual to notice that residual debris from the cork at the mouth of the bottle causes a fair amount of bubbling there (thus causing in turn additional losses of dissolved CO_2). This phenomenon often ceases after one or two services, either by washing or by soaking.

The aim of the following paragraph is to propose a multiparameter modeling that accounts for the major physical parameters that influence the level of dissolved CO_2 found within each flute of a given series (i.e., all along the pouring process of a whole bottle type).

Toward a Multiparameter Modeling. The theoretical model developed in the Modeling section, which provides the concentration c_L of dissolved CO_2 found within the champagne bulk inside the bottle during the pouring process, is the starting point of our discussion.

By replacing in eq 12 the volume $V(t)$ of champagne remaining within the bottle during the pouring process by $V(t) \approx V_0 - v$, eq 12, transforms as

$$\frac{c_L}{c_0} \approx \left(\frac{V_0 - v}{V_0}\right)^{(DS/k\delta)} \tag{13}$$

with v being the total volume of champagne already served during the pouring process.

Equation 13 is indeed particularly useful, since it enables us to follow the concentration c_L of dissolved CO_2 found within a given bottle type, depending on the volume already served from the bottle. The average concentration $[c_L]_n$ of dissolved CO_2 found within the volume of champagne being served into the nth flute of a series of successively poured flutes from a given bottle can therefore easily be accessed with the following relationship

$$[c_L]_n = \frac{1}{v_F}\left[\int_{(n-1)v_F}^{nv_F} c_L dv\right] - \Delta c_L \tag{14}$$

with v_F being the volume of champagne served into a flute (i.e., 100 mL in the present case) and Δc_L being the concentration of dissolved CO_2 lost during the pouring process due to turbulences and bubbles entrapment when champagne invades the flute (see ref 25 for more details about the value of Δc_L depending on the temperature of champagne).

By replacing c_L in eq 14 by its theoretical expression given in eq 13 and by integrating, the average modeled concentration $[c_L]_n$ found within the volume of champagne freshly served into the nth flute, expresses as follows

Table 1. Various Physicochemical and Geometrical Parameters Characteristic of Each Bottle Type Used in This Set of Experiments (at 12 °C)[a]

bottle type	initial volume of champagne within the bottle, V_0 (in mL)	initial concentration of dissolved CO_2 within the bottle (at 12 °C), c_0 (in g L^{-1}), as determined with eq 4	maximal surface offered to gas discharging during the pouring process, S (in cm^2)	total number of flutes successively served per bottle type, n_{max}
half bottle	375	11.3	127.1 ± 0.5	3
standard bottle	750	11.6	191.8 ± 1.1	7
magnum bottle	1500	11.8	250.9 ± 0.9	14

[a]It is worth noting that both the rate k at which champagne escapes from the bottleneck during the pouring process and the thickness δ of the boundary layer near the air/champagne interface were considered as being constant, whatever the bottle type, and equal to 10^{-5} m^3/s and 20 μm (i.e., 2×10^{-5} m), respectively; the maximal surface offered to gas discharging during the pouring process, denoted S, was estimated for each bottle type using the ImageJ 1.45 software (National Institutes of Health, USA [28]). Briefly, the inner side of the bottle was manually outlined on a technical drawing corresponding to each type of bottle. The outlined surface area was then automatically calculated in pixels through ImageJ and then, converted to cm^2.

$$[c_L]_n = \frac{c_0 V_0}{v_F\left(\frac{DS}{k\delta}+1\right)}\left[\left(\frac{V_0 - nv_F}{V_0}\right)^{\left(\frac{DS}{k\delta}+1\right)} - \left(\frac{V_0 - (n-1)v_F}{V_0}\right)^{\left(\frac{DS}{k\delta}+1\right)}\right] - \Delta c_L \quad (15)$$

The aim of the two following paragraphs is to discuss the role of both the bottle type and the temperature, respectively, on the level of dissolved CO_2 found within the successively poured flutes, as decrypted from our multiparameter modeling.

Impact of Bottle Type. Table 1 compiles the various parameters characteristic of each bottle type used in our set of experiments. It is worth noting that both the rate k at which champagne flows from the bottleneck and the thickness δ of the boundary layer near the air/champagne interface were considered as being constant whatever the bottle type. Since the time needed to fill a flute with 100 mL of champagne is about 10 s, the volume flow rate is considered as being on the order of $k \approx 10$ mL $s^{-1} \approx 10^{-5}$ m^3 s^{-1}. Otherwise, and generally speaking, the thickness δ of the boundary layer strongly depends on the mixing conditions and flow patterns close to the interface. For modeling purposes, a thickness δ of 20 μm was retrieved, which corresponds to the order of magnitude of the thickness of the boundary layer under convective conditions for bubble nucleation in champagne glasses.[29]

By replacing in eq 15 each and every parameter by its numerical value (see Table 1 and Abbreviations Used for more details), the average concentration of dissolved CO_2 found within the volume of champagne being served into the nth flute of a series of successively poured flutes can be theoretically determined. The graph displayed in Figure 9 shows the average concentration of dissolved CO_2 found within the successively poured flutes, as theoretically determined with eq 15 for the three bottle types (at 12 °C). Very clearly, the same trends evidenced by our experimental data (displayed in Figure 7) have also been evidenced by our multiparameter modeling.

(i) For a given bottle type, the concentration of dissolved CO_2 found within a flute progressively decreases from the first to the last flute served. Nevertheless, it is worth noting that the modeled concentrations of dissolved CO_2 found within the flutes systematically declines faster, from the first to the last one, than the experimental data. For example, in the magnum, the model forecasts a decline of dissolved CO_2 between the first and the last flute from 8.5 to 5.5 g L^{-1}, whereas the data displayed in Figure 7 show a decline from about 8 to 6 g L^{-1}. In reality, the free air/champagne interface offered to gas discharging first increases during the pouring process (until the volume of champagne within the bottle reaches one-half of the bottle capacity), and then it progressively decreases. Actually, for modeling purposes, the free air/champagne interface was considered as constant and equivalent to the maximal surface offered to gas discharging (see Table 1), which slightly overestimates indeed the losses of dissolved CO_2 during the pouring process (but provides an analytically soluble equation derived in eq 15). Moreover, the hypothetic glug−glug effect is not taken into account in this model, so that the model cannot account for the seemingly lower dissolved CO_2 concentrations found in the first served flutes.

(ii) For a given flute number in a pouring series, the model forecasts a concentration $[c_L]_n$ of dissolved CO_2

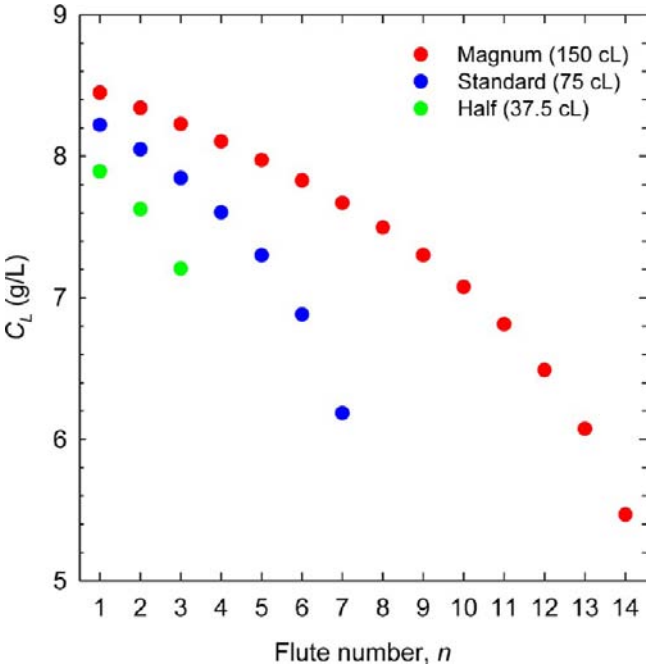

Figure 9. Average concentration of dissolved CO_2 found within the volume of champagne being served into the nth flute of a series of successively poured flute, as theoretically determined with eq 15 for the three bottle types.

systematically higher when it is served from the magnum than from the standard bottle than from the half-bottle (which is clearly consistent with our experimental data shown in Figure 7). For example, experimental data show that the average dissolved CO_2 concentration within the third flute in a series is on order of 7.7, 7.4, and 6.7 g L^{-1} when it is served from the magnum, standard bottle, and half-bottle, respectively. From the taster point of view, this is particularly useful since it means that, for a given flute number in a pouring series, the magnum has a better ability to retain dissolved CO_2 in the liquid phase than the standard bottle, which has a better ability to retain dissolved CO_2 than the half bottle. Very clearly, the higher the bottle volume, the better its buffering capacity with regard to dissolved CO_2 found within champagne during the pouring process (for a given flute number in a pouring series). Nevertheless, every medal has its own reverse. Actually, the model accounts for systematically lower concentrations of dissolved CO_2 within the last flutes of the higher sized bottles. According to the model, the last flute of a whole service holds a concentration c_L of order of 5.5, 6.2, and 7.2 g L^{-1} when champagne is served from a magnum, standard bottle, and half bottle, respectively. Experimentally indeed, dissolved CO_2 concentrations found within the last flute served from the magnum are on order of 0.8 g L^{-1} lower than in the last flutes served from the standard and half bottle, respectively. It seems indeed logical, because the higher the bottle volume, that more time is needed to serve the whole champagne volume (which inevitably impacts the concentration of dissolved CO_2 in the last flutes of a given series served from high-sized bottles). More experiments and especially with higher sized bottles than the magnum, are nevertheless needed to confirm and eventually extend the conclusions of the present article to the service of champagne from higher sized bottles (up to the mythic 15 L Nebuchadnezzar bottle).

Impact of Temperature. It clearly appears from our experimental data displayed in Figure 8 that the higher the temperature of champagne the higher the loss of dissolved CO_2 within the successively poured flutes (from the first to the last one served from a standard 75 cL bottle). Why such a dependence? The diffusion coefficient of the CO_2 molecule denoted D, which rules the diffusion rate through the air/champagne interface as seen in eq 13, is indeed strongly temperature dependent. Actually, D may be approached through the well-known Stokes−Einstein equation as follows

$$D \approx \frac{k_B T}{6\pi\eta a} \tag{16}$$

with k_B being the Boltzmann constant (1.38×10^{-23} J K^{-1}) and a being the characteristic size of the CO_2 molecule's hydrodynamic radius ($a \approx 10^{-10}$ m).

It is worth noting that since the viscosity of champagne is strongly temperature dependent, as seen in eq 1, the diffusion coefficient of dissolved CO_2 molecules is also in turn strongly temperature dependent. By combining eqs 1 and 16 and replacing k_B and a by their numerical values, D finally transforms as

$$D \approx (6.78 \times 10^{-8}) T \exp\left(-\frac{2.81 \times 10^3}{T}\right) \tag{17}$$

Following eq 17, the lower the champagne temperature is, the lower the diffusion coefficient of dissolved CO_2 molecules. Therefore, it is no wonder that the lower the champagne temperature is the lower the loss of dissolved CO_2 found within the bottle during the pouring process. The graph displayed in Figure 10 shows the theoretical temperature dependence of the average concentration c_L of dissolved CO_2 found within the volume of champagne served into the nth flute of a series (for the standard 75 cL bottle). Figure 10 has been drawn by replacing the diffusion coefficient D found in eq 15 by its temperature-dependence relationship given in eq 17. It clearly appears from Figure 10 that the higher the champagne temperature is the lower the average concentration of dissolved CO_2 served within the nth flute of a series, which is self-consistent with the temperature dependence of our experimental data displayed in Figure 8.

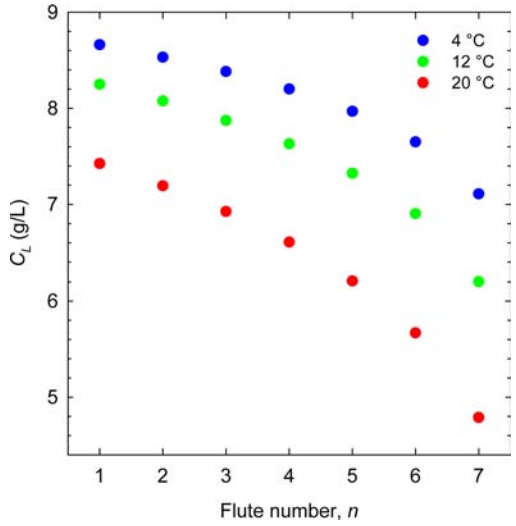

Figure 10. Theoretical temperature dependence of the average concentration of dissolved CO_2 found within the volume of champagne served into the nth flute of a pouring series from the standard 75 cL bottle; this figure has been drawn by replacing the diffusion coefficient D found in eq 15 by its temperature-dependence relationship given in eq 17.

Concentrations of dissolved CO_2 found in successively poured flutes were measured during the service of a given whole champagne bottle type (from the first to the last flute). Three distinct bottle types, namely, a magnum bottle, a standard bottle, and a half bottle, were examined with regard to the level of dissolved CO_2 found within the successively poured flutes. A decreasing trend is observed with regard to the concentration of dissolved CO_2 found within a flute (from the first to the last one of a whole service). Furthermore, for a given flute number in a pouring data series, the concentration of dissolved CO_2 found within the flute decreases as the bottle volume decreases. From the taster point of view, it means that for a given flute number in a pouring series the magnum has a better ability to retain dissolved CO_2 in the liquid phase than the standard bottle, which has a better ability to retain dissolved CO_2 than the half bottle. When it comes to champagne serving, the bottle size definitely does matter. Seemingly, the higher the bottle volume, the better its buffering capacity with regard to

dissolved CO_2 molecules found within champagne during the pouring process. Nevertheless, the higher the bottle volume, the lower the concentration of dissolved CO_2 within the last flute of a pouring series. It seems indeed logical because the higher the bottle volume the more time is needed to serve the whole champagne volume and the more dissolved CO_2 is lost as time proceeds. The impact of champagne temperature (at 4, 12, and 20 °C) on the level of dissolved CO_2 found in successively poured flutes for a given standard 75 cL bottle was also examined. The decreasing trend observed with regard to the concentration of dissolved CO_2 found within the successively poured flutes (from the first to the last one of a whole service) is all the more important as the champagne temperature increases. Our experimental results were discussed on the basis of a multiparameter model that accounts for the major physical parameters that influence the loss of dissolved CO_2 during the service of a whole bottle type. Our model seems in good accordance with tendencies experimentally underscored with regard to both the bottle type and the temperature. In particular, the model accounts for systematically lower concentrations of dissolved CO_2 within the last flutes of the higher sized bottles. More experiments, especially with higher sized bottles than the magnum, are nevertheless needed to confirm and eventually extend the conclusions of the present article to the service of champagne from higher sized bottles (up to the mythic 15 L Nebuchadnezzar bottle).

AUTHOR INFORMATION

Corresponding Author

*Phone/fax: + 333 26 91 88 25. E-mail: gerard.liger-belair@univ-reims.fr.

Funding

Thanks are due to Carinna and Europôl'Agro Institute for financial support and to the Association Recherche Oenologie Champagne Université for moral and financial support.

Notes

The authors declare no competing financial interest.

ACKNOWLEDGMENTS

Thanks are due to champagne Cattier, Pommery, and to Coopérative Nogent l'Abbesse for regularly supplying us with various champagne samples. Authors are also indebted to the Région Champagne-Ardenne, the Ville de Reims, and the Conseil Général de la Marne for supporting our research.

ABBREVIATIONS USED

- a CO_2 molecule's hydrodynamic radius, $\sim 10^{-10}$ m
- c_0 initial dissolved CO_2 concentration found within the champagne bulk within the closed bottle (before pouring), in g L^{-1}
- c_i dissolved CO_2 concentration found within the the air/champagne interface in equilibrium with the gaseous CO_2 in the vapor phase, in g L^{-1}
- c_L dissolved CO_2 concentration found in the liquid phase, in g L^{-1}
- D diffusion coefficient of dissolved CO_2 molecules in the liquid phase, $\sim 1.4 \times 10^{-9}$ m^2 s^{-1}, as determined through ^{13}C nuclear magnetic resonance in a previous work[29]
- J flux of CO_2 moles escaping the free air/champagne interface through invisible diffusion, in mol m^{-2} s^{-1}
- k rate at which champagne escapes from the bottleneck during serving (i.e., $k = dV/dt$), in m^3 s^{-1}
- k_B Boltzmann constant, 1.38×10^{-23} J K^{-1}
- k_H Henry's law constant of CO_2 molecules in champagne, in g L^{-1} bar^{-1}
- m total mass of CO_2 trapped within the bottle, in g
- n index corresponding to the place of a given flute in the series of successive pourings
- P pressure of gaseous CO_2 under the cork, in bar
- R ideal gas constant, 8.31 J K^{-1} mol^{-1}
- S maximal surface offered to gas discharging during the pouring process (see Figure 6), in m^2
- t time, in s
- T temperature, in K
- v total volume of champagne already served during the pouring process of a given bottle type, in L
- v_{HS} volume of the gaseous headspace trapped under the cork, in L (namely, 25 mL in the present case)
- v_F volume of champagne served into each flute, in L (namely, 100 mL in the present case)
- V volume of champagne within the bottle, in L
- V_0 initial volume of champagne found within the bottle (before pouring), in L
- δ thickness of the boundary layer where a gradient of dissolved CO_2 exists, ~ 20 μm (i.e., $\sim 2 \times 10^{-5}$ m)
- γ champagne surface tension, ~ 50 mN m^{-1}
- ρ champagne density, $\sim 10^3$ kg m^{-3}
- η champagne dynamic viscosity, in kg m^{-1} s^{-1}.

REFERENCES

(1) Liger-Belair, G. Nucléation, ascension et éclatement d'une bulle de champagne. *Ann. Phys. (Paris)* **2006**, *31*, 1−133.

(2) Liger-Belair, G. The physics and chemistry behind the bubbling properties of champagne and sparkling wines: A state-of-the-art review. *J. Agric. Food Chem.* **2005**, *53*, 2788−2802.

(3) Liger-Belair, G.; Polidori, G.; Zéninari, V. Unraveling the evolving nature of gaseous and dissolved carbon dioxide in champagne wines: A state-of-the-art review, from the bottle to the tasting glass. *Anal. Chim. Acta* **2012**, *732*, 1−15.

(4) Dessirier, J. M.; Simons, C.; Carstens, M.; O'Mahony, M.; Carstens, E. Psychophysical and neurobiological evidence that the oral sensation elicited by carbonated water is of chemogenic origin. *Chem. Senses* **2000**, *25*, 277−284.

(5) Thurauf, N.; Friedel, I.; Hummel, C.; Kobal, G. The mucosal potential elicited by noxious chemical stimuli with CO_2 in rats: Is it a peripheral nociceptive event? *Neurosci. Lett.* **1991**, *128*, 297−300.

(6) Livermore, A.; Hummel, T. The influence of training on chemosensory event-related potentials and interactions between the olfactory and trigeminal systems. *Chem. Senses* **2004**, *29*, 41−51.

(7) Kleeman, A.; Albrecht, J.; Schöpf, V.; Haegler, K.; Kopietz, R.; Hempel, J. M.; Linn, J.; Flanagin, V. L.; Fesl, G.; Wiesmann, M. Trigeminal perception is necessary to localize odors. *Physiol. Behav.* **2009**, *97*, 401−405.

(8) Meusel, T.; Negoias, S.; Scheibe, M.; Hummel, T. Topographical differences in distribution and responsiveness of trigeminal sensitivity within the human nasal mucosa. *Pain* **2010**, *151*, 516−521.

(9) Chandrashekar, J.; Yarmolinsky, D.; von Buchholtz, L.; Oka, Y.; Sly, W.; Ryba, N. J.; Zucker, C. S. The taste of carbonation. *Science* **2009**, *326*, 443−445.

(10) Dunkel, A.; Hofmann, T. Carbonic anhydrase IV mediates the fizz of carbonated beverages. *Angew. Chem., Int. Ed.* **2010**, *49*, 2975−2977.

(11) Brand, G. Olfactory/trigeminal interactions in nasal chemoreception. *Neurosci. Biobehav. Rev.* **2006**, *30*, 908−917.

(12) Lawless, H.; Heymann, H. *Sensory evaluation of food: principles and practices*; Springer: New York, 2010.

(13) Pozo-Bayon, M. A.; Santos, M.; Martin-Alvarez, P. J.; Reineccius, G. Influence of carbonation on aroma release from liquid

systems using an artificial throat and a proton transfer reaction-mass spectrometric technique (PTR-MS). *Flavour Fragr. J.* **2009**, *24*, 226−233.
(14) Saint-Eve, A.; Déléris, I.; Aubin, E.; Semon, E.; Feron, G.; Rabillier, J.-M.; Ibarra, D.; Guichard, E.; Souchon, I. Influence of composition (CO_2 and sugar) on aroma release and perception of mint-flavored carbonated beverages. *J. Agric. Food Chem.* **2009**, *57*, 5891−5898.
(15) Liger-Belair, G.; Marchal, R.; Jeandet, P. Close-up on bubble nucleation in a glass of champagne. *Am. J. Enol. Vitic.* **2002**, *53*, 151−153.
(16) Liger-Belair, G.; Vignes-Adler, M.; Voisin, C.; Robillard, B.; Jeandet, P. Kinetics of gas discharging in a glass of champagne: The role of nucleation sites. *Langmuir* **2002**, *18*, 1294−1301.
(17) Liger-Belair, G. La physique des bulles de champagne. *Ann. Phys. (Paris)* **2002**, *27*, 1−106.
(18) Liger-Belair, G. The physics behind the fizz in champagne and sparkling wines. *Eur. Phys. J. Spec. Top.* **2012**, *201*, 1−88.
(19) Agabaliantz, G. G. Bases scientifiques de la technologie des vins mousseux. *Bull. O.I.V* **1963**, *36*, 703−714.
(20) Liger-Belair, G.; Villaume, S.; Cilindre, C.; Jeandet, P. Kinetics of CO_2 fluxes outgassing from champagne glasses in tasting conditions: The role of temperature. *J. Agric. Food Chem.* **2009**, *57*, 1997−2003.
(21) Liger-Belair, G.; Villaume, S.; Cilindre, C.; Polidori, G.; Jeandet, P. CO_2 volume fluxes outgassing from champagne glasses in tasting conditions: flute versus coupe. *J. Agric. Food Chem.* **2009**, *57*, 4939−4947.
(22) Liger-Belair, G.; Villaume, S.; Cilindre, C.; Jeandet, P. CO_2 volume fluxes outgassing from champagne glasses: The impact of champagne aging. *Anal. Chim. Acta* **2010**, *660*, 29−34.
(23) Tipler, P.; Mosca, G. *Physics for Scientists and Engineers*; W. H. Freeman: New York, 2003.
(24) Caputi, A.; Ueda, M.; Walter, P.; Brown, T. Titrimetric determination of carbon dioxide in wine. *Am. J. Enol. Vitic.* **1970**, *21*, 140−144.
(25) Liger-Belair, G.; Bourget, M.; Villaume, S.; Jeandet, P.; Pron, H.; Polidori, G. On the losses of dissolved CO_2 during champagne serving. *J. Agric. Food Chem.* **2010**, *58*, 8768−8775.
(26) Incropera, F.; Dewitt, D.; Bergman, T.; Lavine, A. *Fundamentals of Heat and Mass Transfer*; Wiley: New York, 2007.
(27) Clanet, C.; Searby, G. On the glug-glug of ideal bottles. *J. Fluid Mech.* **2004**, *510*, 145−168.
(28) http://imagej.nih.gov/ij.
(29) Liger-Belair, G.; Voisin, M.; Jeandet, P. Modeling nonclassical heterogeneous bubble nucleation from cellulose fibers: Application to bubbling in carbonated beverages. *J. Phys. Chem. B* **2005**, *109*, 14573−14580.
(30) Liger-Belair, G.; Prost, E.; Parmentier, M.; Jeandet, P.; Nuzillard, J.-M. Diffusion coefficient of CO_2 molecules as determined by ^{13}C NMR in various carbonated beverages. *J. Agric. Food Chem.* **2003**, *51*, 7560−7563.